

 Open access • Journal Article • DOI:10.1007/S003400050852

Polarization properties of coherent VUV light at 125 nm generated by sum frequency four wave mixing in mercury — [Source link](#)

Luc Museur, C. Olivero, Damien Riedel, Marie-Claude Castex

Institutions: University of Paris

Published on: 01 Apr 2000 - Applied Physics B (Springer-Verlag)

Topics: Circular polarization, Polarization rotator, Polarization (waves) and Four-wave mixing

Related papers:

- [Four-wave mixing with Rydberg levels in rubidium vapor: Observation of interference fringes](#)
- [Parametric four-wave mixing in Kr.](#)
- [Observation of the two-photon resonant parametric four-wave mixing in the NO C \$2\Pi\$ \(\$v = 0\$ \) state](#)
- [Polarization of signal wave radiation generated by parametric four-wave mixing in rubidium vapor : Ultrafast \(\$\sim 150\$ -fs\) and nanosecond time scale excitation](#)
- [Modulating the multi-wave mixing processes via the polarizable dark states](#)

Share this paper:    

View more about this paper here: <https://typeset.io/papers/polarization-properties-of-coherent-vuv-light-at-125-nm-560odziote>



HAL
open science

Polarization properties of coherent VUV light at 125 nm generated by sum frequency four wave mixing in mercury

Luc Museur, Charles Olivero, Damien Riedel, Marie Claude Castex

► To cite this version:

Luc Museur, Charles Olivero, Damien Riedel, Marie Claude Castex. Polarization properties of coherent VUV light at 125 nm generated by sum frequency four wave mixing in mercury. Applied Physics B - Laser and Optics, Springer Verlag, 2000, 70, pp.499. hal-00276084

HAL Id: hal-00276084

<https://hal.archives-ouvertes.fr/hal-00276084>

Submitted on 28 Apr 2008

HAL is a multi-disciplinary open access archive for the deposit and dissemination of scientific research documents, whether they are published or not. The documents may come from teaching and research institutions in France or abroad, or from public or private research centers.

L'archive ouverte pluridisciplinaire **HAL**, est destinée au dépôt et à la diffusion de documents scientifiques de niveau recherche, publiés ou non, émanant des établissements d'enseignement et de recherche français ou étrangers, des laboratoires publics ou privés.

Polarization properties of coherent VUV light at
125 nm generated by sum frequency four wave mixing
in mercury.

L. Museur, C.Olivero, D.Riedel, M.C. Castex

(Fax: 33 1 49 40 32 00, e-mail: name@lpl.univ-paris13.fr)

Laboratoire de Physique des Lasers

CNRS (UMR 7538), Institut Galilée

Université Paris 13

99 Avenue J.B Clément 93430 Villetaneuse, FRANCE.

July 9, 1999

Abstract

The polarization of the VUV light generated by four-wave sum frequency mixing process $\omega_4 = 2\omega_1 + \omega_2$ in mercury vapor at room temperature is analyzed in detail. Due to the specific two-photon transition used to enhance the nonlinear process, the polarization of the VUV wave is shown to be identical to the polarization of the wave at the frequency ω_2 . In particular, circularly polarized VUV is observed with degree of circular polarization exceeding 0.99.

PACS: 42.65 Pc, 42.25 Ja

1 Introduction.

Vacuum ultra-violet (VUV) light with a high and well known degree of polarization, in the 10 eV range (~ 125 nm), is a powerful tool for a large amount of investigations. Many important properties of various materials may be revealed by experiments using either linearly or circularly polarized VUV radiation. For example, linear polarized VUV light is useful for the study of anisotropic properties of oriented samples [1]. A method such as linear dichroism is extremely sensitive for analyzing differential absorption of oriented molecules [2]. Moreover, for measurement of optical constants, ellipsometry technique is now becoming available to the VUV region [3]. The first reported spectroscopic ellipsometry study above 6 eV was using linearly polarized synchrotron radiation and triple-reflexion polarizers [4]. Energetic polarized light is also convenient to obtain vectorial information on photodissociative excitation processes through measurement of fluorescence anisotropy of excited fragments [5]. It can be used to control the reaction geometry of small encounters when one of the reactants is generated by a photodissociation process [6]. With circularly polarized radiation, fundamental information about electronic structures are accessible. Circular dichroism is an extremely useful tool for investigating the electronic properties of optically active molecules. It is particularly sensitive to the conformation structure of molecules [7, 8] and gives the possibility of obtaining different populations of left vs the right-handed excited molecular states of enantiomers of a chiral molecule [9]. Polarized radiation at 10 eV is also of interest for photoelectron spectroscopy which is highly selective to the state symmetry. Right and left-handed circularly polarized radiation will produce spin-polarized electrons from single crystal and gases [10, 11, 12]. It was also recently demonstrated that photoelectron spectro-microscopy is a powerful method to study the electronic structure and dynamical properties of molecules adsorbed on surfaces [13].

During the last decade, spectroscopic studies with VUV polarized light have been largely stimulated by the development of performant VUV sources either high brightness synchrotron radiation beam lines [14, 15] or coherent nonlinear sources [16, 17, 18, 19]. But to extract useful information, the state of polarization of the VUV light must be accurately

determined. Various optical devices based on reflection [20, 21, 22, 23] or transmission with birefringent material such as MgF_2 [24, 25] (but in that case, at energies lower than the 10.8 eV transparency limit) have been proposed to produce [26] or to probe [27, 28] VUV polarized light. The use of reflection type analyzers usually necessitates a good calibration procedure in the VUV energy region in order to characterize the polarization properties of radiation [29].

Coherent VUV radiation generated by nonlinear frequency mixing presents a number of advantages such as intensity, high resolving power and adjustable polarization state. We present in this paper, a detailed analysis of the polarization properties of VUV light produced at 125 nm by a 4-wave sum-frequency mixing (FWSFM) process $\omega_4 = 2\omega_1 + \omega_2$ in mercury vapor. The dependence of the polarization state of the VUV radiation is studied as a function of the polarization state of the visible wave at frequency ω_2 . The paper is organized as follows. In section 2 we describe the experimental set-up. In section 3 we present the experimental results obtained when the visible fundamental beam (\mathbf{E}_2) is elliptically polarized, the UV beam (\mathbf{E}_1) being kept linearly polarized. In section 4, the results are discussed and analyzed. It is demonstrated that use of a two photon ($\Delta J = 0$) resonant four-wave mixing process leads to a convenient polarized VUV source.

2 Experimental setup.

The laser system, which generates intense pulses of VUV radiation has been described previously in [30]. Briefly, we used only one pulsed dye laser (Quantel TDL50) operating with a mixture of Rh640 and DCM which is pumped by the green output of a doubled Nd : YAG laser (Quantel). The tunable visible output laser beam near 626 nm (ω_2^{-1}) is frequency doubled in a type II KDP crystal ($\omega_1 = 2\omega_2$). Behind the KDP crystal, a "zig-zag" device, composed of two dichroic mirrors (R_{max} for 308 nm) and two right angle prisms, is used to split and recombine the two UV and visible beams. The two collinear laser beams are then focused with an achromatic lens ($f = 38$ cm) in a vapor pressure mercury cell at *room temperature* ($N_{\text{Hg}} \sim 4.10^{13}$ at/cm³) closed by a LiF window (fig.1). With such a specific arrangement it is possible to modify independently the

polarization of the UV (ω_1) and visible (ω_2) beams by introducing different waveplates. The entrance and exit windows of the mercury cell have been installed very carefully in order to avoid stress induced birefringence, which could affect the measurement of the polarization of the VUV. When scanning the dye laser, two VUV emissions are produced by the FWSFM process $\omega_4 = 2\omega_1 + \omega_2$. The first emission at 1251.4 Å is observed when the doubled dye-laser frequency ω_1 is tuned to the two-photon transition $7s^1S_0 \leftarrow 6s^1S_0$ ($2\omega_1 = 63928 \text{ cm}^{-1}$). The second emission at 1250.5 Å is observed when the doubled dye-laser frequency ω_1 is weakly detuned from the two-photon transition $7s^1S_0 \leftarrow 6s^1S_0$ to the blue. The emission intensities are twofold enhanced by resonance effects. A VUV output $I_{\text{vuv}} \approx 10^{12}$ photons/pulse is measured for these two emissions [31].

In the VUV range, transparent birefringent materials are rather scarce and reflection devices are more convenient as polarizers [25]. Also, we used, behind the Hg-cell, a set of two lithium fluoride (LiF) plates at 45° incidence angle which reflects a part of the VUV beam onto a CsI solar-blind photomultiplier. Moreover, for a total rejection of the UV and visible beams, a Lyman α interferential filter is placed in front of the photomultiplier. After amplification, the VUV signal is visualized and stored by a Textronic digitizing oscilloscope. In this configuration, the LiF plates act as polarizers since their reflectivities depend strongly on the polarization state of the VUV incident beam. For an incident angle of 45°, a ratio $R_s/R_p \approx 8.6$ is obtained at 125 nm. In principle, to analyze the polarization of the VUV light we need to rotate the analyzer composed of the LiF plates. Nevertheless, experimentally it is much more convenient to rotate the VUV electric field \mathbf{E}_4 in front of a fixed polarizer rather than to rotate an analyzer in the vacuum chamber. This rotation can be readily achieved by rotating simultaneously, by the same angle $\theta/2$, two half-wave plates L1 and L2 introduced in the "zig-zag". The fundamental fields \mathbf{E}_2 and \mathbf{E}_1 are then rotated by θ . Due to the isotropic nature of the nonlinear medium this is equivalent to rotate directly the VUV field \mathbf{E}_4 by the angle θ . Moreover, a zero-order quarter-wave plate (L3) is used to make elliptical the polarization of the field \mathbf{E}_2 .

3 Results.

Initially, the visible (\mathbf{E}_2) and UV (\mathbf{E}_1) beams are linearly polarized along the vertical (y) and the horizontal (x) axis respectively. We have measured the variation of the VUV intensity reflected by the two LiF plates as a function of the rotation angle ($\theta/2$) of the two half-wave plates L1 and L2 and for different ellipticity ξ of the visible wave, which is modified by using the quarter-wave plate L3. Some typical curves, obtained for the emission at 1251.4 are presented on the figure 2 (the field \mathbf{E}_1 is kept linearly polarized). If the fundamental beams are both linearly polarized, the VUV wave is then necessarily linearly polarized. In these conditions, the variation of the VUV intensity on the detector is sinusoidal (fig.2.a) and the ratio of maximum to minimum signal characterizes the polarization analyzer efficiency. The maxima, which correspond to a s polarized VUV wave, are observed for $\theta = 0$ or π , and indicate that the VUV field \mathbf{E}_4 is parallel to \mathbf{E}_2 . When the visible field \mathbf{E}_2 becomes elliptically polarized ($\xi \neq 0$) the signal still varies sinusoidally, but the amplitude of the oscillations decreases and the curves are shifted of an angle ψ to the right (fig.2.b) or to the left (fig.2.c) depending on the sign of the ellipticity ξ . This means, on one hand, that the polarization of the VUV becomes elliptical and, on the other hand, that the major axis of the ellipse is inclined by an angle ψ with respect to the vertical direction. We have determined this angle ψ by fitting the variation of the VUV intensity as function of θ with the curve $I_{\text{VUV}} = (I_{\text{max}} - I_{\text{min}}) \cos^2(\theta + \psi) + I_{\text{min}}$. The values of ψ obtained for different values of the ellipticity ξ are presented on the figure 3. Finally, we have analyzed the polarization of the VUV light when the visible wave is circularly polarized ($\xi = \pm 1$). The result is presented on the figure 2.d. After the fit procedure the residual degree of linear polarization is given by [32]:

$$P_{\text{lin}} = \frac{I_{\text{max}} - I_{\text{min}}}{I_{\text{max}} + I_{\text{min}}}. \quad (1)$$

Assuming that the VUV wave is completely polarized, its degree of circular polarization is then determined using [32]:

$$P_{\text{circ}} = (1 - P_{\text{lin}}^2)^{1/2}. \quad (2)$$

In these conditions we have measured $P_{\text{circ}} = 99.9\%$ for the emission at 1251.4 Å and $P_{\text{circ}} = 99.8\%$ for the second emission at 1250.5 Å.

4 Discussion.

The polarization of the VUV wave generated by FWSFM can be readily analyzed using the nonlinear third order susceptibilities $\chi^{(3)}$. Let us consider two electric fields \mathbf{E}_1 and \mathbf{E}_2 propagating in an isotropic nonlinear medium along the direction $\hat{\mathbf{z}} = \hat{\mathbf{x}} \wedge \hat{\mathbf{y}}$ ($\hat{\mathbf{x}}$, $\hat{\mathbf{y}}$ and $\hat{\mathbf{z}}$ are three orthogonal unit vectors). We shall assume the field \mathbf{E}_1 linearly polarized while the field \mathbf{E}_2 is elliptically polarized, and we shall write :

$$\mathbf{E}_1 = E_1 \exp(-i\omega_1 t) \hat{\mathbf{x}} + cc \quad (3a)$$

$$\mathbf{E}_2 = \frac{E_2}{1 + \xi^2} \left(\xi (1 + i) \hat{\mathbf{x}} + (1 - i\xi^2) \hat{\mathbf{y}} \right) \exp(-i\omega_2 t) + cc \quad (3b)$$

where ξ is the ellipticity of the beam at the frequency ω_2 . These two fields interact with the nonlinear medium to generate, by FWSFM, an electric field \mathbf{E}_4 at the frequency $\omega_4 = 2\omega_1 + \omega_2$. The amplitude of the nonlinear polarization associated to this process is given by [33] :

$$P_{4\mu} = \varepsilon_0 \sum_{\gamma} \chi_{\mu\alpha\alpha\gamma}^{(3)}(-\omega_4; \omega_1, \omega_1, \omega_2) E_{1\alpha} E_{1\alpha} E_{2\gamma} \quad (4)$$

where $\chi^{(3)}$ is the third order nonlinear susceptibility and $\mu, \gamma = [x, y]$. In these conditions, it is straightforward to write the electric field at the frequency ω_4 . We obtain the relations:

$$\mathbf{E}_4 = (E_{4x} \hat{\mathbf{x}} + E_{4y} \hat{\mathbf{y}}) \exp(-i\omega_4 t) + cc \quad (5a)$$

$$\text{with } E_{4x} \propto \frac{E_1^2 E_2}{2(1 + \xi^2)} \xi (1 + i) \chi_{xxxx}^{(3)}(-\omega_4; \omega_1, \omega_1, \omega_2) \quad (5b)$$

$$\text{and } E_{4y} \propto \frac{E_1^2 E_2}{2(1 + \xi^2)} (1 - i\xi^2) \chi_{yyxy}^{(3)}(-\omega_4; \omega_1, \omega_1, \omega_2) \quad (5c)$$

where the four non zero independent elements of $\chi^{(3)}$ are related by the relation

$$\chi_{xxxx}^{(3)} = \chi_{yyxy}^{(3)} + \chi_{xyxy}^{(3)} + \chi_{xxyy}^{(3)} \quad (6)$$

From the previous expressions it is clear that the polarization of the electric field \mathbf{E}_4 is completely controlled by the polarization of the fundamental field \mathbf{E}_2 . Thus, if the field \mathbf{E}_2 is linearly polarized along $\hat{\mathbf{y}}$ ($\xi = 0$) then, in agreement with the observations (fig.2.a), the field \mathbf{E}_4 is also linearly polarized in the same direction ($E_{4x} = 0$). In the more general case ($\xi \neq 0$) the field \mathbf{E}_4 is elliptically polarized. In particular, when the wave \mathbf{E}_2 is

right-handed circularly polarized ($\xi = +1$), the VUV wave is right-handed elliptically polarized with the ellipticity $\xi_4 = +\chi_{yxxy}^{(3)}/\chi_{xxxx}^{(3)}$. These remarks are, of course, consistent with the conservation of the angular momentum in the FWSFM process $\omega_4 = 2\omega_1 + \omega_2$. Experimentally, we have observed a circular VUV wave when the field \mathbf{E}_2 was circularly polarized (fig.2.d). This means that $\chi_{xxxx}^{(3)} = \chi_{yxxy}^{(3)}$ and therefore that $\chi_{xyxy}^{(3)} = \chi_{xxyy}^{(3)} = 0$. This is a consequence of the two-photon resonance used to enhance the FWSFM process. By writing the various polarization vectors in the complex spherical basis ($\hat{\mathbf{e}}_0 = \hat{\mathbf{z}}$, $\hat{\mathbf{e}}_{\pm 1} = \mp(\hat{\mathbf{x}} + i\hat{\mathbf{y}})/\sqrt{2}$), the two-photon resonant third order susceptibilities can be factorized in two parts. The first part gives explicitly the relation between the electric fields, the second part contains the physics of the atom in the form of reduced matrix elements and $6j$ symbols. With use of spherical tensor techniques the third order susceptibility is proportional to [34, 35]:

$$\chi^{(3)}(-\omega_4; \omega_1, \omega_1, \omega_2) \propto \sum_K (2K+1)^{-1} \langle \gamma_f J_f \| \alpha_{-\omega_2; \omega_4}^{(K)} \| \gamma_g J_g \rangle^* \langle \gamma_f J_f \| \alpha_{\omega_1; \omega_1}^{(K)} \| \gamma_f J_f \rangle \theta^{(K)} \quad (7)$$

where the label K denotes a spherical-tensor rank, and $\theta^{(K)}$ is the angular factor :

$$\theta^{(K)} = (-1)^K (\hat{\mathbf{e}}_2 \otimes \hat{\mathbf{e}}_4^*)^{(K)} \cdot (\hat{\mathbf{e}}_1 \otimes \hat{\mathbf{e}}_1)^{(K)} \quad (8)$$

In the relation (7), f and g represent the levels involved in the two-photon transition, Ω_{fg} is a transition frequency, $\alpha_{\omega_i; \omega_j}$ is the first-order transition hyperpolarisability, $\hat{\mathbf{e}}_i$ is the polarization unit vector of the field \mathbf{E}_i and \otimes stands for a tensor product. The rank K is subjected to the selection rule such that (J_f, J_g, K) should obey the triangle rule [34, 35]. In our experiment the levels f and g are of 1S_0 symmetry ($J_g = J_f = 0$). In this case, $K = 0$ and the tensor products in the relation (8) are reduced to the usual scalar product. The angular factor $\theta^{(0)}$ can be readily calculated for the various components of the nonlinear susceptibility $\chi^{(3)}$. Thus, for the components $\chi_{xyxy}^{(3)}(-\omega_4; \omega_1, \omega_1, \omega_2)$ and $\chi_{xxyy}^{(3)}(-\omega_4; \omega_1, \omega_1, \omega_2)$ the polarization vectors of the fields \mathbf{E}_4 and \mathbf{E}_2 are $\hat{\mathbf{e}}_4 = \frac{1}{\sqrt{2}}(-\hat{\mathbf{e}}_{+1} + \hat{\mathbf{e}}_{-1}) = \hat{\mathbf{x}}$ and $\hat{\mathbf{e}}_2 = \frac{i}{\sqrt{2}}(\hat{\mathbf{e}}_{+1} - \hat{\mathbf{e}}_{-1}) = \hat{\mathbf{y}}$, therefore $\theta^{(0)} = 0$ and $\chi_{xyxy}^{(3)} = \chi_{xxyy}^{(3)} = 0$. At the reverse, for the elements $\chi_{xxxx}^{(3)}(-\omega_4; \omega_1, \omega_1, \omega_2)$ and $\chi_{yxxy}^{(3)}(-\omega_4; \omega_1, \omega_1, \omega_2)$, we have $\hat{\mathbf{e}}_2 = \hat{\mathbf{e}}_4$. In this case $\theta^{(0)} = 1/3$ and, from the relation (6), we obtain $\chi_{xxxx}^{(3)} = \chi_{yxxy}^{(3)}$. In these conditions, the polarization of the VUV wave should be strictly identical to the

polarization of the wave \mathbf{E}_2 . In particular, the angle ψ should correspond to the rotation angle of the quarter wave plate L3 from an origin given by the vertical direction. The function $\psi = \tan^{-1}(\xi)$ is plotted on the figure 3 and is in good agreement with the experimental points. Finally, let us note that in a large number of nonlinear experiments, with use of metallic vapor or rare gases as nonlinear media, four-wave mixing enhancement is obtained with $J_f = 2 \leftarrow J_g = 0$ two-photon resonance [36]. In this case $K = 2$ and the angular factor $\theta^{(2)}$ is always different of zero. This imply that $\chi_{xyxy}^{(3)} = \chi_{xxyy}^{(3)} \neq 0$. Therefore, in these experiments, if the two-photon transition is excited with linearly polarized light, the production of circularly polarized VUV light not possible.

5 Conclusion.

We have analyzed in detail the polarization of the VUV light generated by FWSFM $\omega_4 = 2\omega_1 + \omega_2$ in mercury vapor at room temperature. Due to the specificity of the two-photon resonance used to enhance the nonlinear process, we show that the polarization of VUV wave \mathbf{E}_4 corresponds exactly to the polarization of the visible wave \mathbf{E}_2 . In particular, we observe circularly polarized VUV with degree of polarization better than 99%. This allows a full control of the VUV polarization, which could be a great advantage for future applications of this VUV source in surface science [37].

References

- [1] K. Nagayama, T. Miyamae, R. Mitsumoto, H. Ishii, Y. Ouchi and K. Seki: *J. Elect. Spect Rel. Phen* **78**, 407 (1996)
- [2] J. H. Jaffe, H. Jaffe and K. Rosenheck: *Rev. Sci. Instr* **38**, 935 (1967)
- [3] N. Kandaka, M. Yuri, H. Fukutani, T. Koide and T. Shidara: *Rev. Sci. Instrum* **63**, 1450 (1992)
- [4] J. Barth, R.L. Johnson, M. Cardona, D. Fuchs and A.M. Bradshaw: *Phys. Rev. B* **41**, 3291 (1990)
- [5] M. Kono and K. Shobatake: *J. Chem. Phys* **102**, 5966 (1995).
- [6] K-H Gericke, C. Kreher and J.L Rinnenthal: *J. Phys. Chem A* **101**, 7530 (1997).
- [7] W. Curtis Johnson: *Ann. Rev. Phys. Chem* **29**, 93 (1978).
- [8] A. Gedanken and M. Levy: *Rev. Sci. Instrum.* **48**, 1661 (1977)
- [9] A. Salam and W.J. Meath: *Chem. Phys. Lett* **277**, 199 (1997)
- [10] D.T. Pierce and F. Meier: *Phys. Rev.* **13**, 5484 (1976)
- [11] Ch. Keckenkamp, P. Schafers, G. Schonhense and U. Heinzman: *Proc. 7th Int. Conf on VUV Radiation Physics, Jerusalem*, 115 (1983)
- [12] B. Schmiedeskamp: *Proc. VUV X, Paris*, 49 (1992)
- [13] T. Munakata and T. Kasuya: *Jap. J. Appl. Phys.* **28**, 1677 (1989)
- [14] E. Vescovo, H.J. Kim, Q.Y Dong , G. Nintzel, D. Carlson, S. Hubert and N.V. Smith: *Synchrotron Rad. News* **12**, 10 (1999)
- [15] H. Onuki: *Nuclear instr. Methods in Phys. Research A* **246**, 94 (1986)
- [16] P. Antoine, A. L'Huillier, M. Lewenstein, P. Salieres and B. Carre: *Phys. Rev A* **53**, 1725 (1996)

- [17] D. Schuze, M. Dorr, G. Sommerer, J. Ludwig, P.V. Nickles, T. Schlegel, W. Sandner, M. Drescher, U. Kleineberg and U. Heinzmann: Phys. Rev A **57**, 3003 (1998)
- [18] R. Irrgang, M. Drescher, F. Gierschner, M. Spieweck and U. Heinzmann: Meas. Sci. Technol **9**, 422 (1998)
- [19] K. Tsukiyama, M. Tsukakoshi and T. Kasuya: Opt. Com **81**, 327 (1991)
- [20] E.S. Gluskin: Rev. Sci. Instrum **63**, 1523 (1992).
- [21] T. J. McIrath: J. Opt. Soc. of America A **58**, 506 (1968)
- [22] H. Metcalf and J. C. Baird: Appl. Opt. **5**,1407 (1966)
- [23] W.R. Hunter: Appl. Opt. **17**, 1259 (1978)
- [24] H. Eichmann, A. Egbert, S. Nolte, C. Momma, B. Wellegehausen, W. Becker, S. Long and J.K. McIver: Phys. Rev. A **51**, R3414 (1995)
- [25] N. Damany, J. Romand and B. Vodar: *Some aspects of vacuum ultraviolet radiation* (Pergamon, Oxford, 1974)
- [26] W.E. Westerveld, K. Becker, P .W. Zetner, J.J. Corr and J.W. McConkey: Appl. Opt. **24**, 2256 (1985).
- [27] P. Zetner, K. Becker, W.B. Westerveld and J.W. McConkey: Appl. Opt. **23**, 3184 (1984)
- [28] G. Rosenbaum, F. Feuerbacher, R.P. Godwin and M. Skibowski: Appl. Opt. **7**, 1917 (1968)
- [29] M. Uhrig, S. Hornemann, M. Klose, K. Becker and G.F Hanne: Meas. Sci. Technol **5**, 1239 (1994)
- [30] L.Museur, W.Q. Zheng, A.V. Kanaev and M.C. Castex: IEEE J of Select Topics **1**, 900 (1995)
- [31] D. Riedel: Thèse de L'université Paris 13 (1998)

- [32] M.Born and E.Wolf: *Principles of Optics* (Pergamon Press New York 1964)
- [33] R.W.Boyd: *Nonlinear optics* (Academic Press, New york 1992)
- [34] D.C. Hanna, M.A Yuratich and D. Cotter: *Non linear optics of free atoms and molecules*. (Springer series in optical sciences, berlin, Heidelberg 1979)
- [35] M.A Yuratich and D.C. Hanna: J Phys B **9**, 729 (1976).
- [36] W.Jamroz and B.P. Stoicheff: *Progress in optics XX* (edited by E.Wolf, North-Holland 1983)
- [37] D. Riedel and M.C. Castex: Appl. Phys. A to be published (1999).

Figures captions.

Figure 1: Experimental setup. The Glan prism is used to obtain a better linear polarization of the visible wave E_2 .

Figure 2: Variation of the VUV intensity at 1251.4 \AA with respect to twice the rotation angle $\theta/2$ of the half-wave plates L1 and L2. The angle ψ characterizes the inclination of the major axis of the VUV with respect to the vertical direction (see text).

Figure 3: Variation of the angle ψ with respect to the ellipticity ξ of the visible wave E_2 . The line represents the function $\psi = \tan^{-1}(\xi)$.

Fig.1

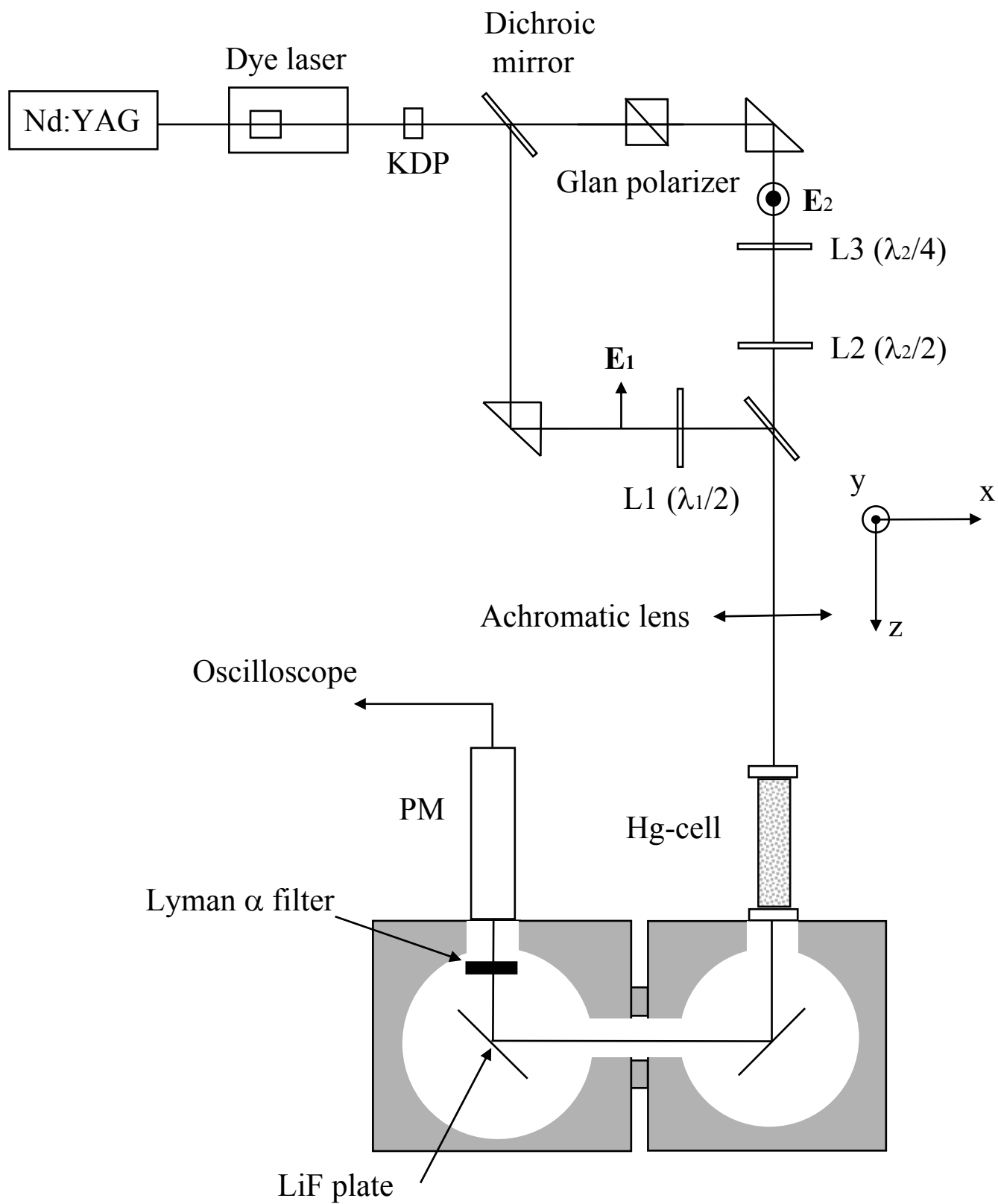


Fig.2

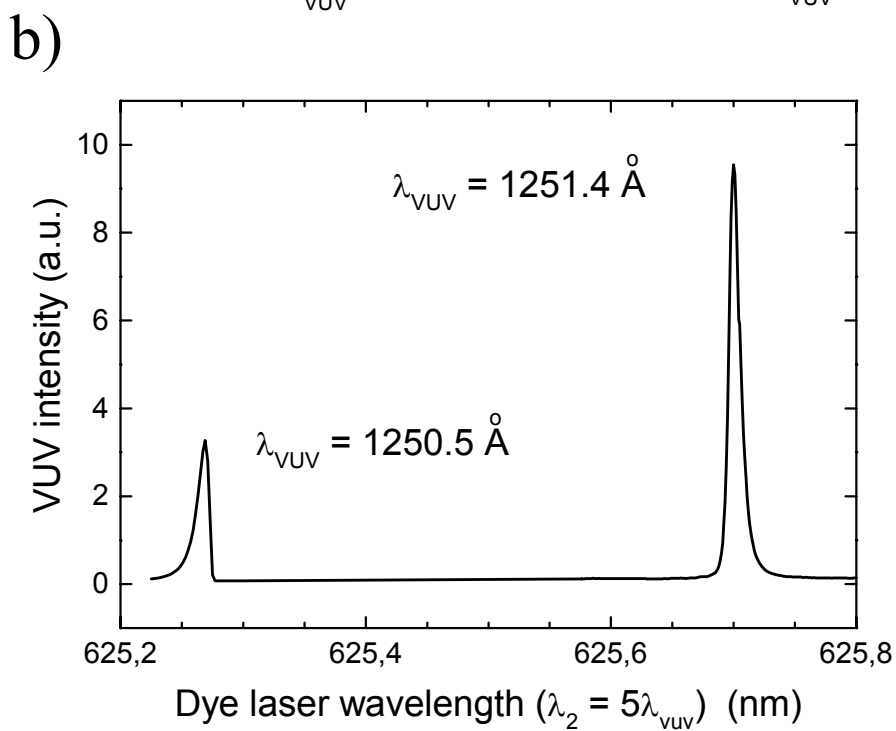
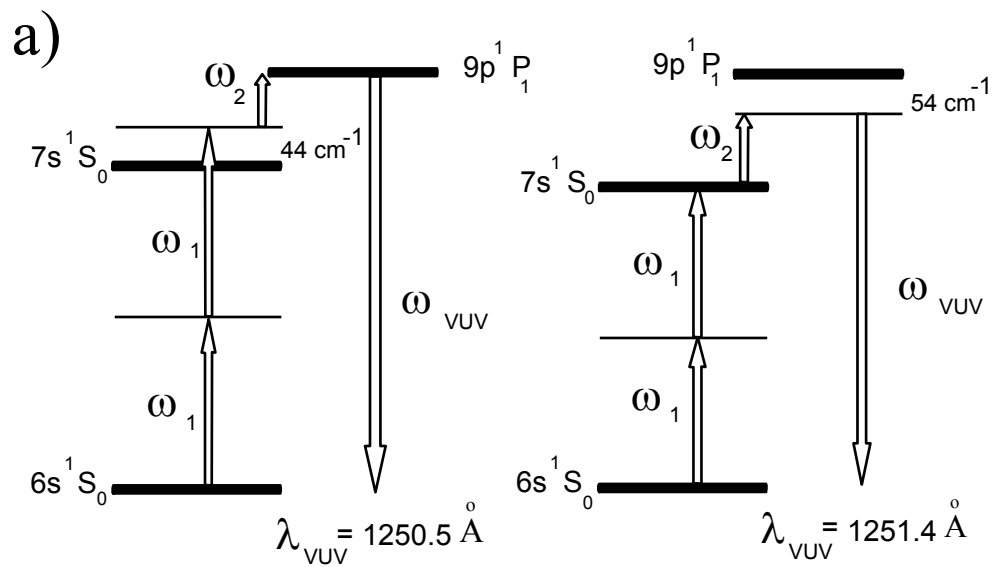
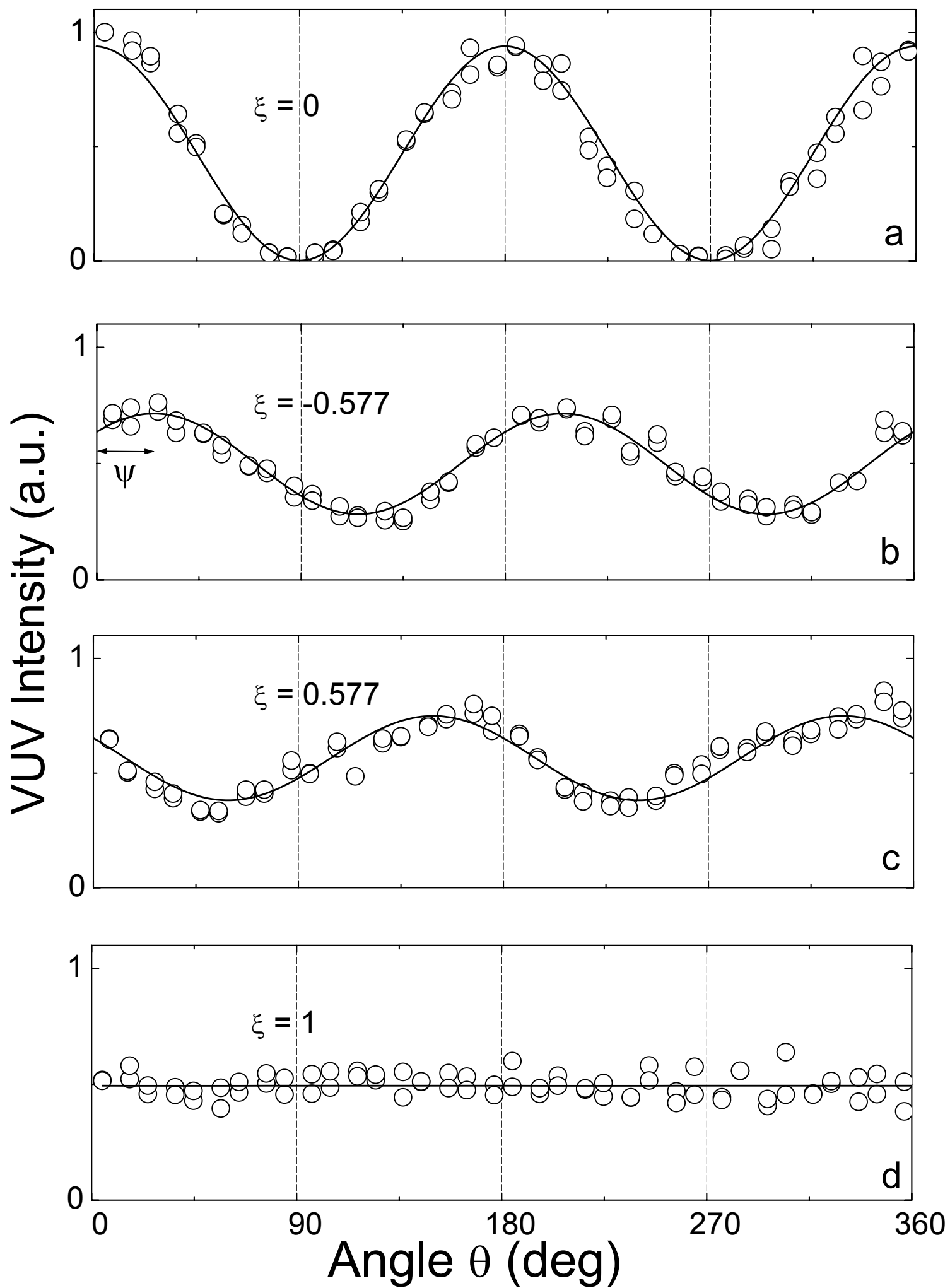


Fig. 3



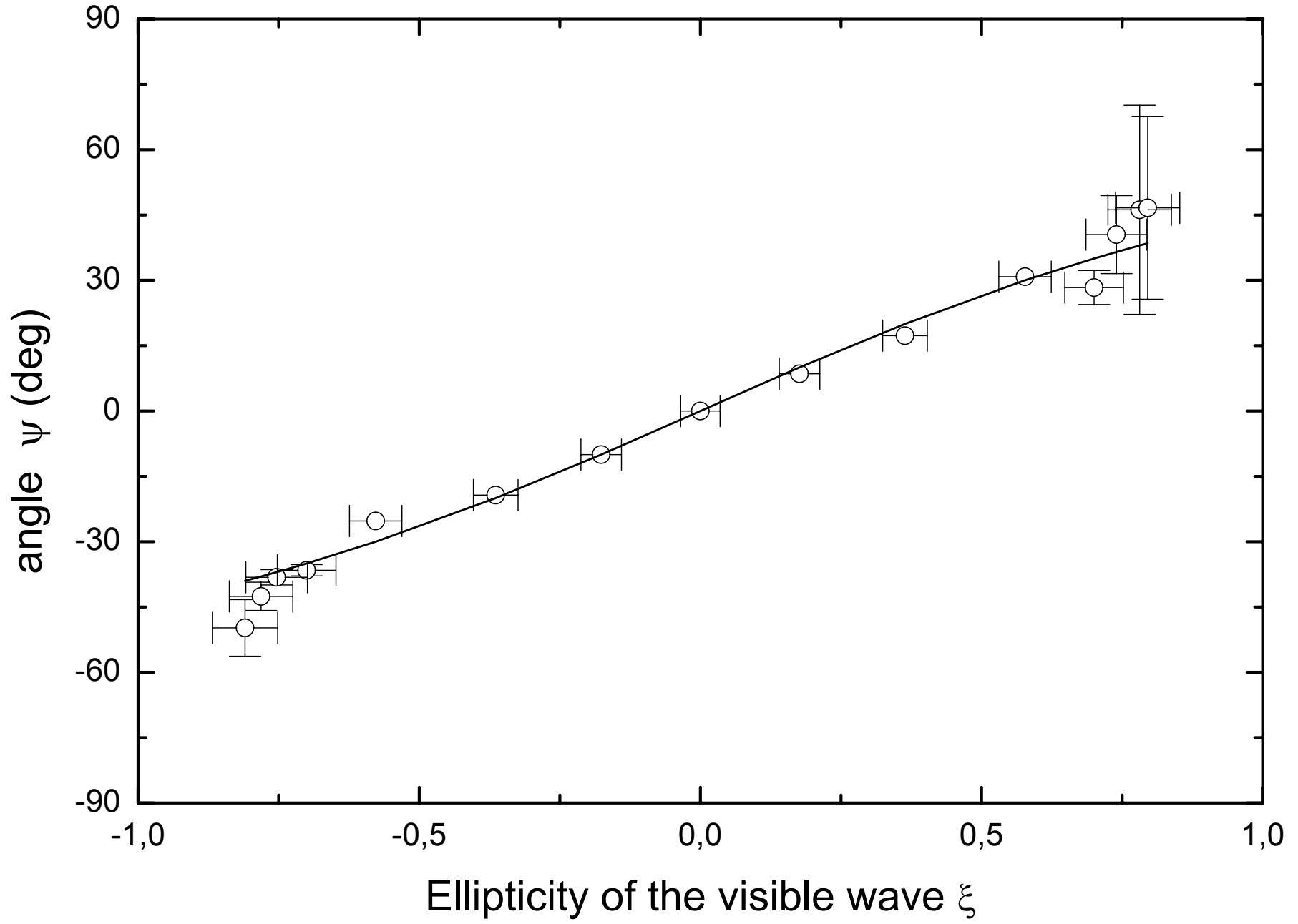


Fig. 4